Clustering and Precipitation Processes in Microalloyed Aluminium Alloys(APFIM/FIM)

Sci. Rep. RITU A44 (1997) pp. 241-251
No. 2, March 1997

Clustering and Precipitation Processes in Microalloyed Aluminium Alloys

Simon P. Ringer[a], Christopher R. Hutchinson[b], Kazuhiro Hono[c], Ian J. Polmear[a] and Toshio Sakurai[d]

[a] *Department of Materials Engineering, Monash University, Clayton 3168, Victoria, Australia*
[b] *Department of Materials Science and Engineering, The University of Virginia, Charlottesville VA 22903, USA*
[c] *National Research Institute for Metals, 1-2-1 Sengen, Tsukuba, 305, Japan*
[d] *Institute for Materials Research, Tohoku University, Sendai 980-77, Japan*

(Received January 31, 1997)

Recent progress in understanding the origins of hardening in Al-1.7Cu-0.01Sn (at. %) and Al-1.1Cu-1.7Mg-(0.1Ag, 0.3-0.5Si) (at. %) microalloyed alloys is presented. The results of systematic studies involving atom probe field ion microscopy in conjunction with transmission electron microscopy indicate that the precipitation processes depend to a considerable degree upon the nature of pre-precipitate clustering reactions which occur early in the decomposition of the solid solution. Furthermore, it is shown that the presence of these co-clusters can influence significantly the alloy properties.

KEYWORDS: atomic clustering, precipitation, light alloys, transmission electron microscopy, atom probe field ion microscopy.

1. Introduction

In age hardened alloys, rational design of microstructure requires an understanding of the mechanisms of the decomposition of solid solutions, atomic clustering and precipitate nucleation. This paper reviews the results arising from an international research program, involving the use of atom probe field ion microscopy (APFIM) and transmission electron microscopy (TEM) in the study of a range of commercially important Al-Cu-Mg based alloys.

Unlike intermetallic alloys such as those based on (e.g.) Ni_3Al, where the effects of microalloying are described reasonably using thermodynamic modelling, the phase relationships in metallic-multicomponent Al alloys are incompletely described. This, and the tendency for the formation of metastable phases, has led to difficulties in making predictions of the effects of alloying on precipitate nucleation. Although a generalised thermodynamic model for precipitation nucleation has been available for some time, little is known about the actual atomic processes involved. Therefore, a primary consideration in carrying out the work reported here has been to make direct observations of these processes and characterise the effects of selected microalloying.

2. Experimental

Table 1 details the composition of the alloys studied.

Table 1. Alloys Studied

ALLOY	COMPOSITION (at. %)
1	Al-1.7Cu-0.01Sn
2	Al-1.1Cu-1.7Mg
3	Al-1.1Cu-1.7Mg-0.1Ag
4	Al-1.1Cu-1.7Mg-0.25Si
5	Al-1.1Cu-1.7Mg-0.1Ag-0.25Si

*IMR, Report No. 2088

These alloys were cast into book molds, homogenised at 525 °C for ~ 72 h. and scalped (5 mm from each face). Samples (~5 x ~10 x ~10 mm) were machined for hardness testing, whilst some material was cold rolled to sheet for TEM studies. Samples for APFIM were spark machined from the bulk to 0.3 x 0.3 x 10 mm or obtained from material drawn to wire. Solution treatment was carried out at 525 °C for 30 min in either salt or Ar atmospheres, followed by cold water quenching. Elevated temperature ageing was performed in an oil bath and hardness monitored using a standard Vickers hardness indentor under a load of 5 kg. Samples for APFIM and TEM were prepared using standard electropolishing techniques[1,2]. The energy compensated time-of-flight APFIM instrumentation used here has been described elsewhere[3,4]. Atom probe analysis was performed at ~ 30 K, in ultrahigh vacuum (10^{-11} Torr). A pulse fraction of 15% was used in all analyses. Analyses were typically performed with ~0.5 nm spatial resolution in the lateral direction and atomic layer resolution in the depth direction. Approximately 10^5 atoms were collected per specimen to ensure reliable statistics. The FIM images were obtained using either Ne gas at around 30 K, or He gas at 20 K. A Philips CM20 (200 kV) TEM at Monash University and a Philips CM12 (120 kV) at Tohoku University were used in the present studies.

3. Review: Alloy 1

3.1 Previous Work

Trace additions of Cd, In and Sn are well known for their effects in modifying ageing in Al-Cu alloys[5]. These elements reduce or inhibit natural ageing by retarding GP-zone formation. This behaviour has been attributed to a preferential interaction between the trace element and quenched-in vacancies that would normally be available to assist diffusion of the solute Cu atoms[6]. This conclusion

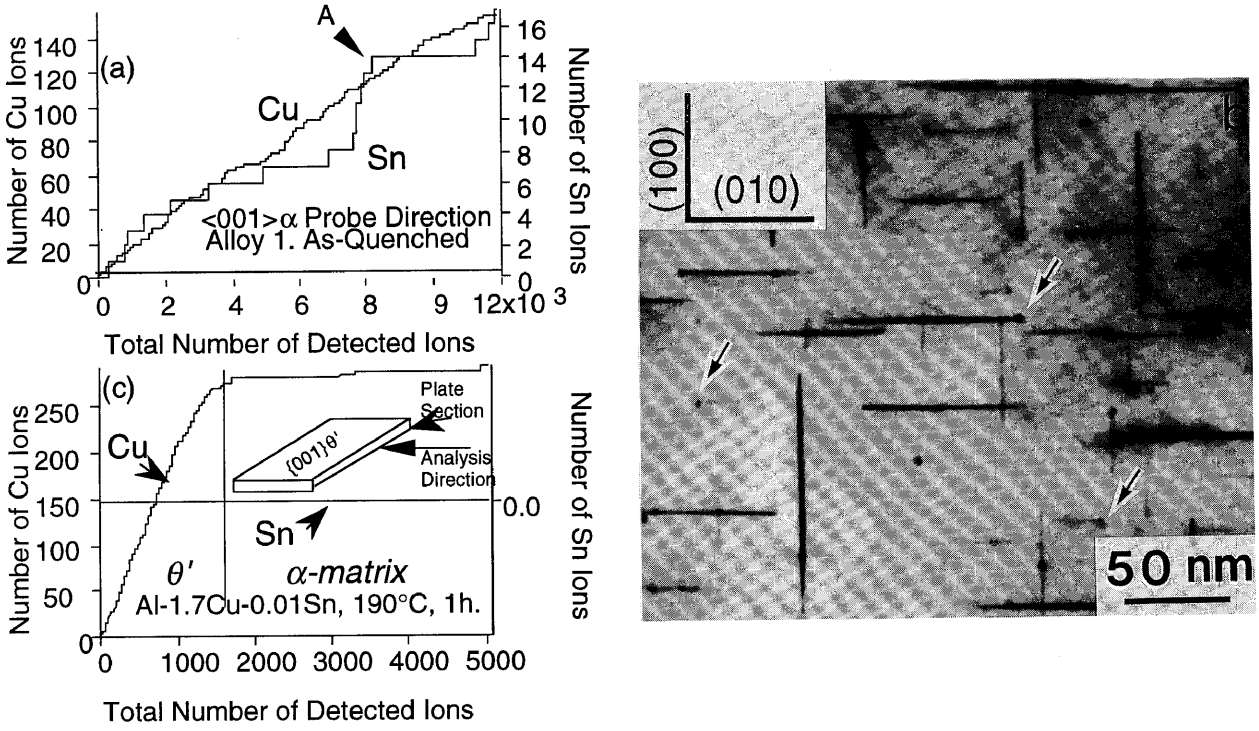

Figure 1. (a) APFIM ladder plot from alloy 1 in as-quenched condition, showing Sn cluster (A). (b) BF TEM micrograph of the alloy aged 1h. at 190°C showing the θ' phase, which appears to be nucleated at the sites of small Sn-particles (arrowed). (c) Ladder plot from atom probe analysis of the rim of a θ' precipitate. Sn appears to be absent from the particle/matrix interface.

is supported by calculations that suggest the binding energy between a vacancy and a Sn atom is 0.2 eV greater than that existing between a vacancy and a Cu atom[7], and by TEM observations which show that these trace elements reduce the size of dislocation loops in quenched alloys[8, 9]. On the other hand, these trace elements increase both the rate and extent of hardening in Al-Cu alloys aged at temperatures in the range 100 to 200 °C[5, 10]. Comparisons between binary and ternary alloys have shown that, whereas these elements suppress the formation of the phase θ''[11], they stimulate a finer and more uniform dispersion of the semi-coherent phase θ'[12]. This change occurs without altering the crystal structure of θ'[11, 12], but opinions differ concerning the mechanisms involved. One hypothesis is that the trace elements are absorbed at the θ'/matrix interfaces resulting in a lowering of the interfacial energy required to nucleate θ'. This explanation was first proposed by Silcock et al.[11] to account for weak X-ray reflections (designated "p-diffractions") that were observed during the early stages of ageing. This proposal received indirect experimental support from calorimetric measurements by Boyd and Nicholson[13] and TEM observations by Sankaren and Laird[14] who claimed to detect what they referred to as Sn (Cd or In) segregates and precipitates in association with the θ' particle/matrix interface. An alternative explanation is that the trace elements facilitate heterogeneous nucleation of θ' either directly at Sn (Cd or In) particles[15], or indirectly at the dislocation loops mentioned above[8, 9].

3.2 Results and Discussion

Figure 1(a) shows an integrated concentration depth profile, or ladder plot, obtained from the as-quenched samples of alloy 1. The diagram shows the number of solute atoms plotted against the total number of atoms collected during atom probe analysis. The slope of each plot corresponds to the local solute concentration in the sample and it is immediately obvious that the Sn atoms are not homogeneously distributed in the Al matrix. Rather they appear as discrete clusters such as at A in Fig. 1(a). Moreover, the result suggests that these clusters are composed of Sn atoms and there is no evidence of enrichment of Cu at their locations. Occasional clusters of Cu atoms were also observed but these appeared to be fewer in number and not spatially correlated with the Sn clusters.

Ageing at 190 °C for 1 h. results in rapid precipitation of fine (~5 nm diameter), approximately spherical particles, which atom probe analysis and microbeam electron diffraction showed to be β-Sn (I4/mcm) oriented such that $(100\}_{Sn}$ // $(111)_{\alpha}$, $[010]_{Sn}$ // $[112]_{\alpha}$[16]. As indicated in Fig. 1(b), θ' precipitates were often found associated with these particles suggesting that they had provided sites at which heterogeneous nucleation of θ' could occur. The

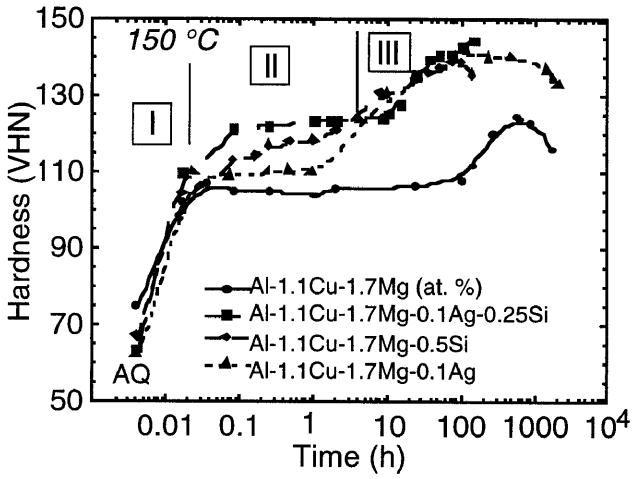

Figure 2. Hardness-time plot for Al-1.1Cu-1.7Mg (at. %) aged at 150 °C, showing the effect of additions of 0.1 at. % Ag and 0.5 at. % Si. In all cases, hardening progresses through three distinct stages.

Sn particles appeared to be incoherent with the Al matrix since they were visible only through diffraction and structure factor contrast and no contrast effects suggestive of coherence strains were observed in tilting experiments. It is apparent that the Sn-particles are in contact with the narrow, incoherent planes of θ'. This is similar to the observation made in an Al-Cu-Zr-alloy by Kanno and Ou[17] in which θ' nucleated at incoherent particles of the compound Al_3Zr. APFIM was also used to determine whether or not Sn atoms were segregated at the θ'/matrix interfaces and separate selected area analyses were performed across both the coherent broad face of the θ' plates and across the rim or edge. Results for the latter analysis are shown in Fig. 1(c) for the alloy aged 1h. at 190 °C, which is approaching peak hardness (~3h.). It is clear that no Sn has segregated to this interface and the same result was obtained across the broad face of the platelets.

These results appear to give strong support to the proposal by Kanno et al.[15] that Sn (Cd or In) facilitates precipitation of θ' at elevated temperatures by providing heterogeneous sites at which nucleation occurs. For alloy 1, the actual nucleation process would seem to involve:

- Rapid vacancy assisted formation of clusters of Sn atoms during, or immediately after quenching. Evidence for the preferential interaction between trace elements and vacancies has already been mentioned and it is also relevant to note that the diffusion rate of Sn in Al may exceed that of Cu by at least two orders of magnitude[18],
- Precipitation of Sn particles,
- Heterogeneous nucleation of θ' on Sn particles. Here it is suggested that it is the incoherent rim or edge of the θ' plates which nucleate, and that this occurs at those surfaces of the incoherent Sn particles which will allow growth of θ' along $\{001\}_\alpha$ planes.

4. Review: Alloy 2

4.1 Previous Work

The phenomenon of age hardening was first discovered in an Al-Cu-Mg alloy by Wilm in Berlin in 1906[19]. This work led to the development of the well known wrought alloy Duralumin which was quickly adopted in Germany for structural members of Zeppelin airships and for the Junkers F13 passenger aircraft that first flew in 1919. These materials remain as one of the two major classes of aluminium alloys used for aircraft construction worldwide (2000 series). Here we present a new interpretation of the origin of hardening in these important alloys.

Isothermal ageing of most Al-Cu-Mg alloys over a wide temperature range (100 to 240 °C) reveals several interesting features which are illustrated in Fig. 2 for the high-purity composition Al-1.1%Cu-1.7%Mg (at. %):

- hardening occurs in two distinct stages separated by a plateau during which time the hardness may remain constant for many hours[20, 21],
- the first stage of hardening occurs very rapidly and is largely complete within 60 sec,
- some 60% of the total hardening during ageing (peak hardness minus the hardness measured immediately after quenching from the solution treatment temperature) occurs during this rapid first stage.

The last two features are not widely realised, particularly in commercially heat treated alloys, because accurate values of as-quenched (AQ) hardness are often not determined.

The first stage of hardening in Al-Cu-Mg alloys has generally been attributed to the formation of Guinier-Preston zones comprised of copper and magnesium atoms (often known as GPB zones), although the structure and chemistry of GPB zones remains poorly defined. Evidence for the existence of these zones and their characteristics is based on interpretations of weak diffraction effects arising from diffuse X-ray scattering in alloys aged for times corresponding to various stages along the hardness plateau[22, 23, 24]. Bagaryatsky[23] considered the zones to be associated with short range ordering along the $\{100\}_\alpha$ planes. Later, Silcock[24] proposed that the zones formed along the $<100>_\alpha$ directions as small cylinders estimated to be 1 to 2 nm in diameter and with lengths ranging from 4 to more than 8 nm, depending on quenching rate. Subsequent X-ray diffraction[25] and high resolution transmission electron microscopy (HRTEM)[26] studies of these zones have not added significantly to this understanding.

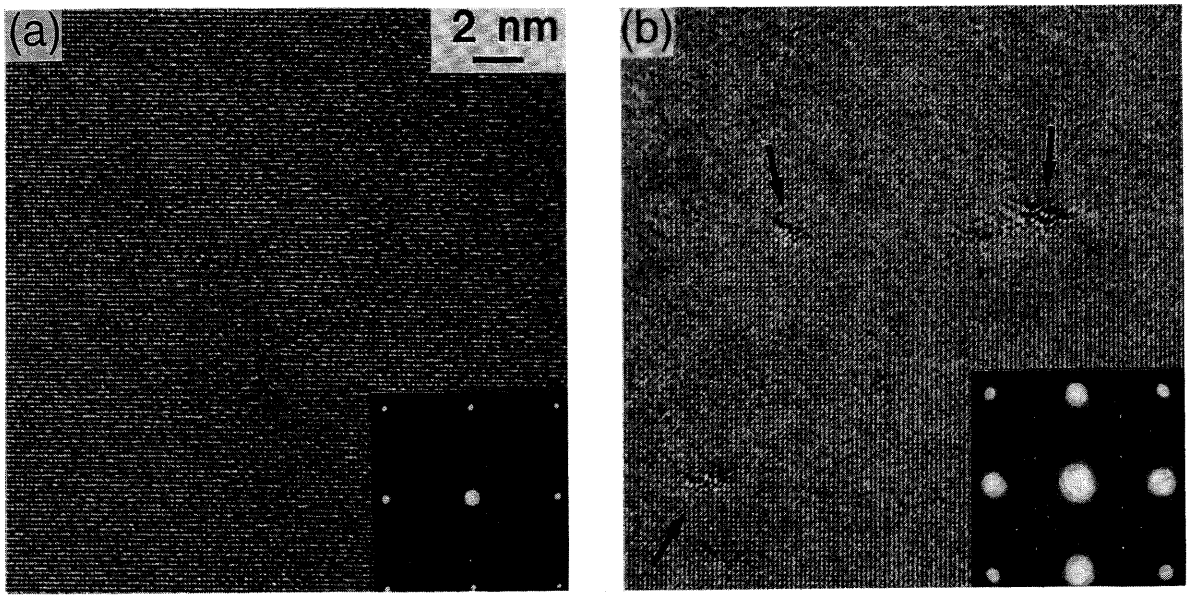

Figure 3. HRTEM images of the Al-1.1%Cu-1.7%Mg (at. %) aged (a) 1 h. and (b) 500 h. at 150 °C, showing GPB zones end-on to the electron beam (arrowed). Corresponding SAED patterns are shown inset.

4.2 Results and Discussion

The present work revealed that something of a dilemma exists when describing the results of a characterisation of these Al-Cu-Mg alloys. This was because neither TEM nor HRTEM show any evidence of GPB zones until ageing had proceeded for times close to the second stage of hardening (Fig. 2). This behaviour is illustrated in Fig. 3(a) for an Al-1.1Cu-1.7Mg (at. %) alloy aged for 1 hour at 150 °C. Here, lattice images obtained by HRTEM have failed to reveal any contrast effects associated with a zone-type structure. In fact, these HRTEM images were unchanged from the AQ condition. Moreover, the inset SAED pattern shows little or no evidence of effects other than the matrix. What are believed to be GPB zones, because of the presence of diffuse streaks in SAED patterns and contrast features in HRTEM images, were not observed until ageing for times close to the second rise in hardness and their appearance close to peak hardness is shown in Fig. 3(b). Evidence for the source of the rapid early hardening has therefore been sought by recourse to the technique of APFIM.

A FIM micrograph of the AQ microstructure of the alloy is provided in Fig. 4(a). The bright spots correspond to Cu atoms or clusters, since this element images brightly in FIM images of Al alloys, whereas Mg would be expected to evaporate more easily and images darkly[27]. These images did suggest the possibility that fine, localised clusters had formed (arrowed) and this interpretation was supported by the atom probe analyses. The plots in Fig. 4(b) are concentration-depth profiles for Cu and Mg in which the dotted lines represent the standard deviations, 2σ, around the mean compositions. This analysis reveals the presence of individual clusters of copper and magnesium atoms (arrowed) which are not spatially correlated. However, ageing for 5 min., during which time the hardness has increased from the quenched value of ~67 VHN to the plateau value of ~100 VHN in less than 60 sec., has resulted in significant co-clustering of copper and magnesium atoms. The corresponding FIM image is shown in Fig. 5(a) and reveals the presence of numerous bright spots (arrowed) which are fine-scale clusters containing Cu atoms. A typical analysis of a cluster is best shown in an integrated concentration-depth profile, (Fig. 5(b)), in which the number of solute atoms detected is plotted as a function of the total number of atoms. The slope of each profile then corresponds to the average local concentration and the coincident, abrupt changes that are observed in the levels of copper and magnesium indicates the presence of pre-precipitate co-clusters of these atoms.

In order to evaluate statistically both the possibility and relative degree of co-segregation of Cu and Mg atoms, contingency table analysis was performed on the raw atom probe data. Results summarising these calculations are shown in Fig. 5(c), where the chi-square distribution is represented and values of the experimental statistic are plotted for AQ samples (*case A*) and samples aged 5 min. at 150 °C (*case B*). The experimental statistic may be used to test the null hypothesis that the Cu and Mg are distributed randomly. This statistic was derived by comparing the experimental and expected frequency of Cu and Mg atoms detected together from blocks of 50 atoms, over a total of ~ 10^5 atoms, in the usual way as described elsewhere[1]. Clearly, results for *cases A* and *B* are different, with *case A* lying within the null hypothesis region. However, results for *case B* show that the null

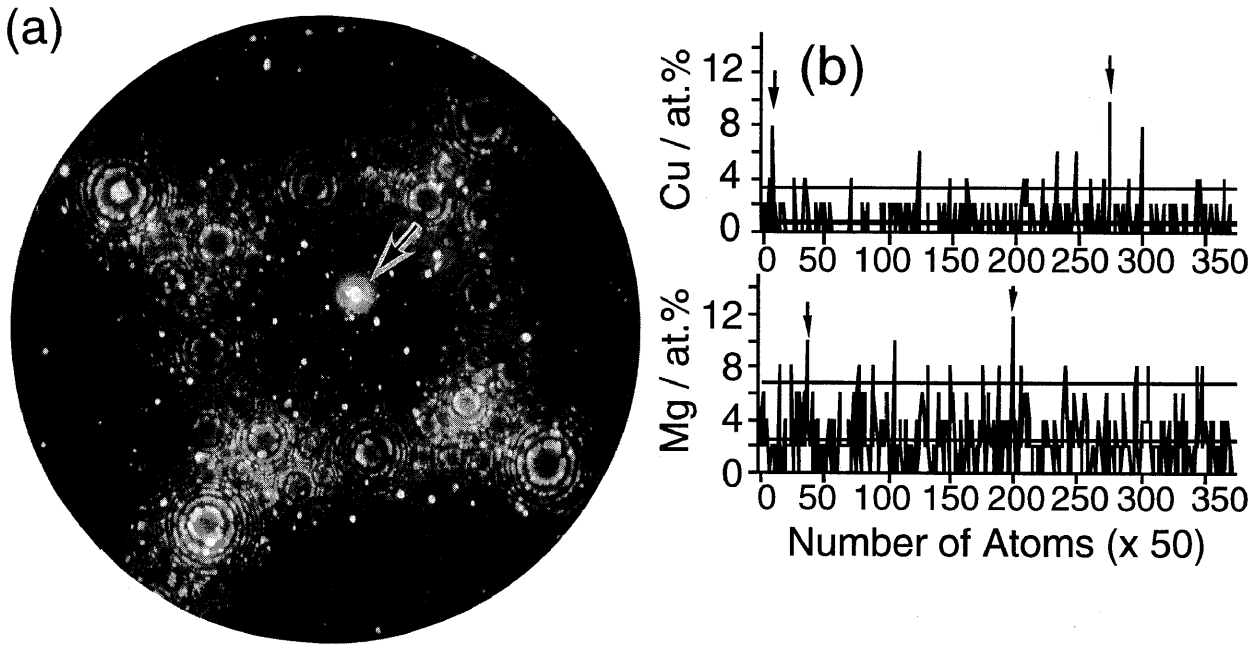

Figure 4 . Results for the Al-1.1%Cu-1.7%Mg (at. %) alloy in the AQ condition, showing (a) He FIM image (b) atom probe concentration-depth profiles for Cu and Mg.

hypothesis must be rejected and that Cu and Mg have a preferred interaction at the 0.025 level of significance.

The clusters are regarded as being distinct from zones, in that their shape, size, composition, degree of order, orientation and structure are less defined than that of a zone. Therefore, their detection by electron microscopy or X-ray diffraction is very difficult, since there are few if any contrast mechanisms available. This is accentuated by the small size of the clusters, which is typically around 10-50 atoms. Moreover, it is likely that these solute clusters typically have a high vacancy content, as both Cu and Mg have positive interactions with vacancies[28, 29]. Based on the FIM image contrast (compare Figs. 4(a) and 5(a)), atom probe data such as that in Fig. 5(b) and statistical evaluations of large volumes of atom probe data, it thus seems that the rapid early hardening observed in the alloy arises from the presence of these co-clusters rather than actual GPB zones.

Clustering prior to the formation of GP zones was recently observed in Al-Cu-Mg(-Ag) alloys with high Cu:Mg ratios[30], but it did not cause significant hardening. Pre-precipitate clustering has also been observed in Al-Mg-Si alloys[31]. We therefore propose the term *cluster hardening* to describe the phenomena reported here. Based on the hardening characteristics[21], it is likely that this occurs in most other Al-Cu-Mg alloys and we suggest that the actual hardening process can be seen as an exaggerated or *super* form of solid solution strengthening.

Although it is to be expected that the GPB zones do form at the sites of Cu-Mg co-clusters, the fact that they are not observed until near to the end of the hardness plateau, and are present at peak hardness (Fig. 3(b)), suggests that their major contribution to age hardening actually occurs during the second, rather than the first stage of hardening. Moreover, it implies that the accepted mechanism of precipitation hardening in these Al-Cu-Mg alloys needs to be modified.

5. Review: Alloys 3-5

5.1 Previous Work

It has been shown that additions of Ag and Si greatly affect the age hardening characteristics of Al-Cu-Mg alloys by modifying the nucleation of precipitates[21, 32]; Fig. 2 shows the effects of microalloying with Ag and Si on the change in hardness as a function of ageing time at 150 °C. In all cases, it is seen that hardening proceeds through three distinct stages. The initial rapid rise in hardness (stage I) is followed by a change in slope, which in some alloys corresponds to a hardness plateau, suggestive of an incubation period (stage II) before a second rise towards peak hardness and overageing (stage III).

As first noted by Polmear[32], the effect of Ag is to significantly increase the magnitude of the first stage of hardening and improve the mechanical properties at peak hardness. Microstructural examination revealed that Ag additions stimulate precipitation of a finely dispersed metastable precipitate, thought to be a cubic T phase, rather than the rod or lath-like S phase found in the Ag-free ternary alloys[21]. However, recent work[33] has shown that this phase, which forms as platelets on $\{111\}_\alpha$ planes, has a hexagonal structure. This phase was designated X,

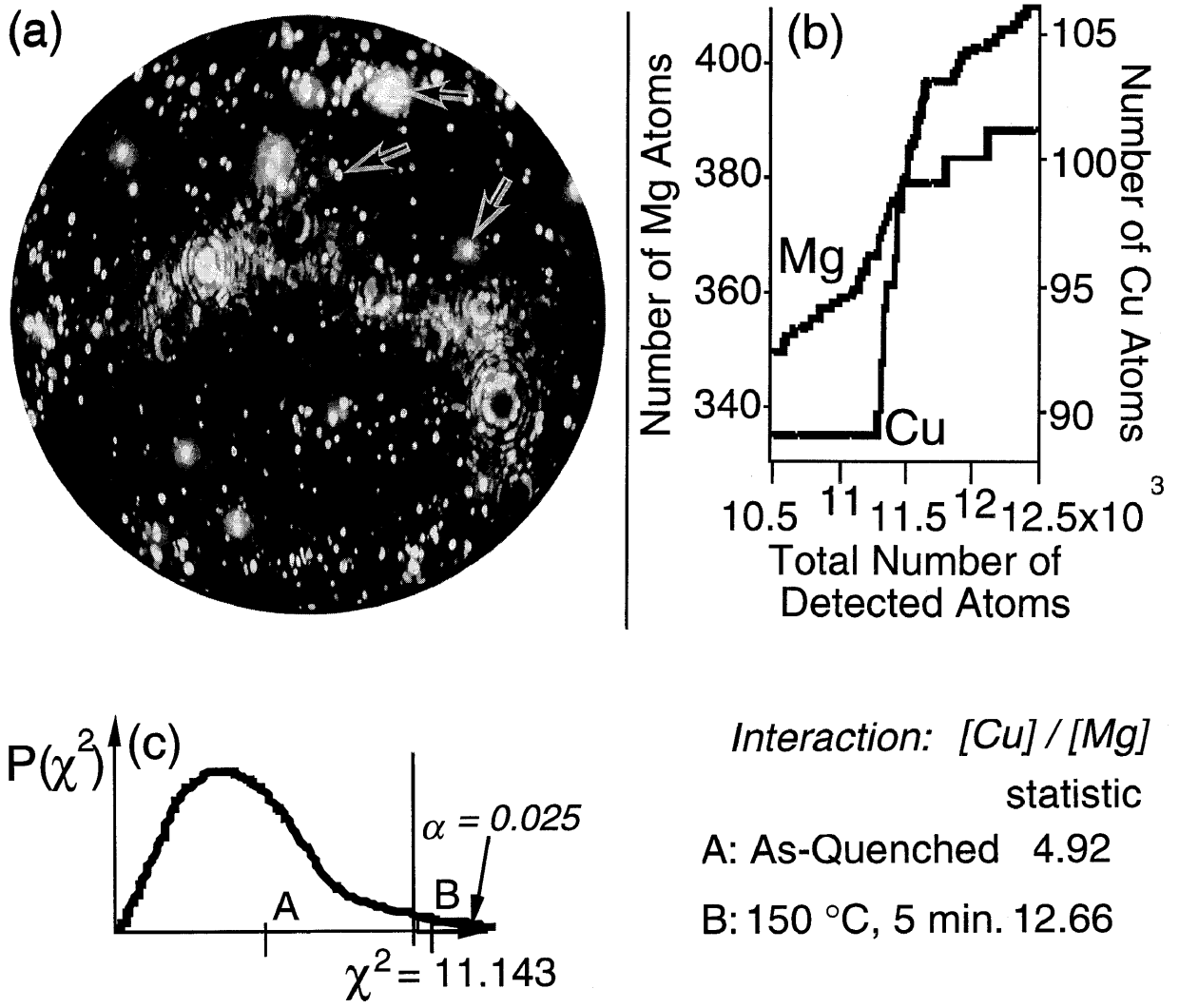

Figure 5. APFIM results for Al-1.1%Cu-1.7%Mg (at. %) alloy aged 5 min. at 150 °C. (a) He FIM image. (b) Integrated concentration-depth profiles for Cu and Mg, showing localised co-clustering. (c) Summary of results from a statistical test of the null hypothesis that Cu and Mg are randomly distributed. We accept the null hypothesis in case A, and reject the null hypothesis in case B at the 0.025 level of significance.

but, as it is metastable, it is proposed to refer to it as X'. This will also distinguish the hexagonal phase from the orthorhombic X phase that has been reported in AA2124 type Al-Cu-Mg alloys[34].

The effect of Ag in promoting a $\{111\}_\alpha$ plate-like phase with at least hexagonal symmetry in this alloy is consistent with the effect of similar additions to Al-Cu-Mg based alloys having higher Cu:Mg ratios, where other $\{111\}_\alpha$ plate-like precipitate phases occur, such as Ω[35] and T_1[36]. On the other hand, no detailed microstructural work has been performed on Ag+Si containing alloys in the α + S phase field, although as noted from the hardening results in Fig. 2, the effects of Ag and Si appear to be somewhat additive[21]. Here, attention is drawn to three aspects of the precipitation processes in these microalloyed alloys. The first is to examine the rapid hardening reaction, Fig. 2, by studying material aged for short times and comparing this to the as-quenched structure. The second concerns the composition of the $\{111\}_\alpha$ phase X' in the Al-1.1Cu-1.7Mg-0.1Ag alloy. In particular, the possibility and nature of segregation of Ag to this phase was examined since Ag has been detected in association with other $\{111\}_\alpha$ phases in Ag modified Al-Cu-Mg alloys[37, 38, 39, 40]. Finally, it was intended to characterise the effect of combined additions of Ag and Si in the peak hardness microstructure of a quinary alloy Al-1.1Cu-1.7Mg-0.1Ag-0.3Si alloy.

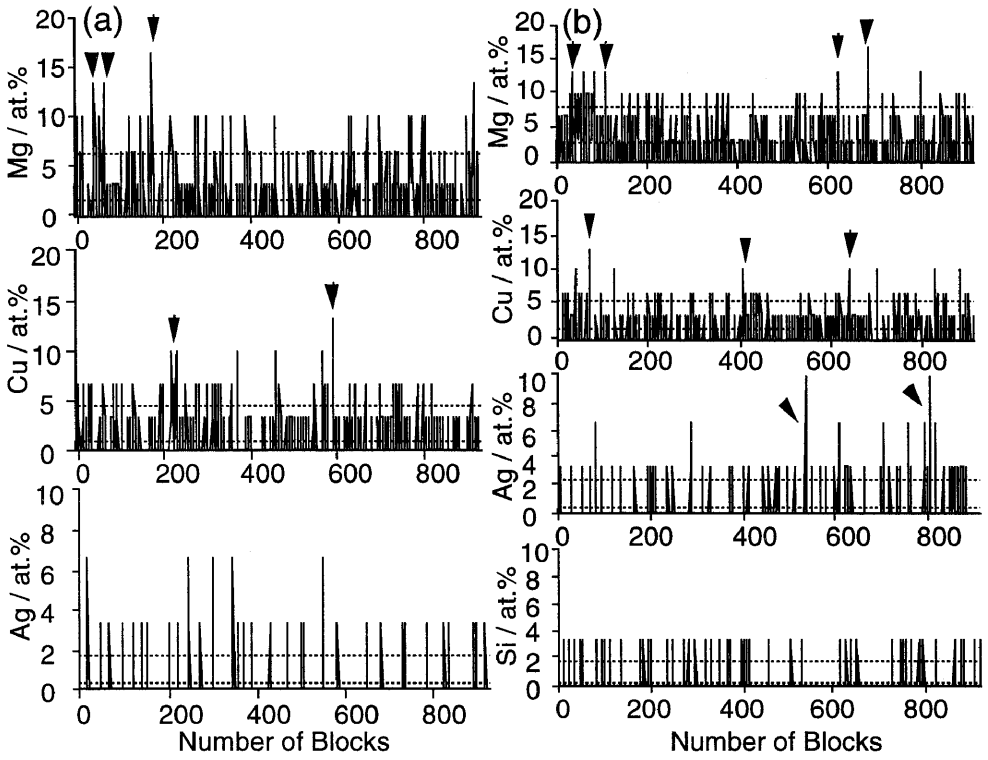

Figure 6. Atom probe analysis of (a) Al-1.1Cu-1.7Mg-0.1Ag and (b) Al-1.1Cu-1.7Mg-0.1Ag-0.25Si (at.%) in the as-quenched state. The concentration-depth profiles were obtained with the probe hole over the $\{110\}_\alpha$ pole.

5.2 Results and Discussion

Figs. 6(a) and (b) compare the results of atom probe analyses of the Si free and Si containing Al-Cu-Mg-Ag alloy, respectively, in the as-quenched condition. The data is in the form of concentration-depth profiles, where atomic concentration is plotted as a function of depth, normalised into blocks of 30 atoms. The dotted lines represent the standard deviation, 2σ, around the mean composition. Clustering of Mg and occasionally Cu atoms was seen with Ag and Si more uniformly distributed. In both cases, these clusters were usually of atoms of the same species and in common with recent studies of as-quenched Al alloys, no co-clustering was detected in the as-quenched state[16, 30].

Figs. 7(a) and (b) compare atom probe concentration-depth profiles of the Si free and Si containing alloys after ageing at 150 °C for 5 min. As seen in Fig. 2, this ageing time is concomitant with a large increase in hardness, marking the transition between stage I and stage II of the hardening process. Results from the Si-free alloy, Fig. 7(a), show evidence for the formation of Mg-Ag co-clusters (arrowed). This result is rather similar to that reported in recent atom probe analyses of an Al-1.7Cu-0.25Mg-(0.1Ag) alloy[30], where the formation of Mg-Ag co-clusters preceded the precipitation of the $\{111\}_\alpha$ Ω phase. In that case, the formation of the Mg-Ag clusters was linked to the formation of Ω, since these elements are known to segregate to the α-Ω interface during plate growth[39, 41]. It is likely that the Mg-Ag clusters reported here are closely linked to the formation of the $\{111\}_\alpha$ X' phase and this is further examined below. Also evident in Fig. 7(a) are numerous Mg-clusters, some of which are correlated spatially with local Cu enrichment. Since the Mg concentration in the alloy is 1.7 at.%, the formation of such clusters is not surprising and the localised Mg-enrichments are clearly seen by comparison to the as-quenched result in Fig. 2(a). The rapid rise in hardness is almost certainly linked to the formation of these various clusters, which would act as finely distributed pinning centers for dislocation movement.

Fig. 7(b) indicates that the kinetics of clustering and precipitation are clearly accelerated by the addition of Si as anticipated from the results in Fig. 1. Two dominant effects were noted: the first was the presence of precipitates rich in Cu and Mg, which contain traces of Ag and Si. The second, less frequently observed effect, was the presence of Cu-rich clusters or precipitates, which usually showed little or no evidence of enrichment by other elements. The formation of such precipitates suggests that the Si addition may increase the free vacancy content of the alloy, facilitating faster solute diffusion. Evidence for this is taken from the Cu profiles, which show that the Si addition causes greater enrichment of Cu in both types of precipitates than corresponding results in the Si-free alloy.

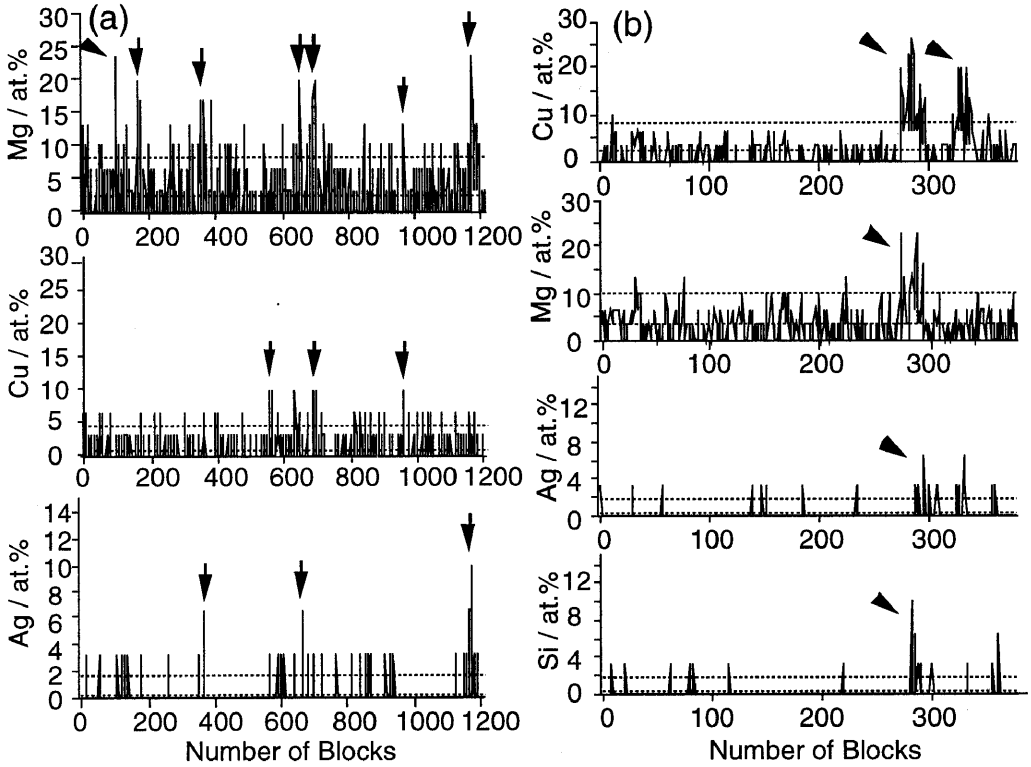

Figure 7. Atom probe analysis of (a) Al-1.1Cu-1.7Mg-0.1Ag and (b) Al-1.1Cu-1.7Mg-0.1Ag-0.25Si (at.%) after ageing for 5 min. at 150 °C. The concentration-depth profiles were obtained with the probe hole over the $\{110\}_\alpha$ pole.

It is seen that the local concentration exceeds 20 at.%, and hardening in this case is attributed to these precipitates,although detailed phase identification must await further TEM examination.

Fig. 8(a-b) shows the results of atom probe analysis of the Al-1.1Cu-1.7Mg-0.1Ag alloy aged at 200 °C for 1 h. Previous work has shown that the microstructure here comprises of a fine and uniform dispersion of the $\{111\}_\alpha$ X' platelet[21]. The analysis was performed with the probe hole near the $\{111\}_\alpha$ pole and it is seen that at least two X' precipitates were cut by the cylinder of analysis. The concentration-depth profile in Fig. 4(a) shows clearly that Ag is associated with the $\{111\}_\alpha$ X' phase. To better assess the precipitate composition and to elucidate the nature of the association of Ag, an integrated concentration-depth profile is provided in Fig. 4(b), together with a schematic representation of the analysis mode. Here, the number of solute atoms detected is plotted as a function of the total number of atoms and thus the slope of each profile corresponds to the local average-solute concentration. The concentration of Cu was generally higher than that of Mg, and Al was the major constituent of the phase if we assume that the probe hole was smaller than the broad facet of the precipitate. The composition of X' was determined to be 20-25 at.% Cu, 15-25 at.% Mg and 50-65 at.% Al implying an Al:Cu:Mg ratio of approximately 2:1:1. The integrated concentration-depth profile also shows that Ag is contained inside the X' precipitate. It is likely that Ag is associated with these precipitates as a result of the Mg-Ag co-clusters detected at the early stages of precipitation. Given that there is < 2% misfit strain normal to the habit plane[33], there is probably less need for Ag to modify the particle/matrix interface than in the case of Ω, where the misfit >9%. Only recently[30] has atom probe analysis confirmed earlier proposals[21, 32] of a preferred Mg-Ag interaction in Al alloys by systematic comparisons between Ag-free and Ag-containing alloys. On this basis, it seems likely that Ag should also be found in the precipitate, since Mg is one of the main constituents of the X' phase.

Fig. 9(a) is a $<110>_\alpha$ BF TEM micrograph of the peak hardness microstructure of the Al-1.1Cu-1.7Mg-0.1Ag-0.3Si (at. %) alloy after ageing for 14 h. at 200 °C and the corresponding SAED pattern is provided in Fig. 9(b). The BF image reveals the presence of fine-scale rod-like precipitates elongated parallel to the $<001>_\alpha$ direction. Another set of precipitate traces is also evident, parallel to the $\{111\}_\alpha$ planes. In common with other $\{111\}_\alpha$ precipitates observed in Al alloys, the SAED patterns possess reflections at 1/3 and 2/3 $\mathbf{g}\{220\}_\alpha$ positions. These as yet unidentified $\{111\}_\alpha$ precipitates were present in the peak hardness microstructures of samples aged at 200 °C. The aspect ratio of the $\{111\}_\alpha$ precipitates

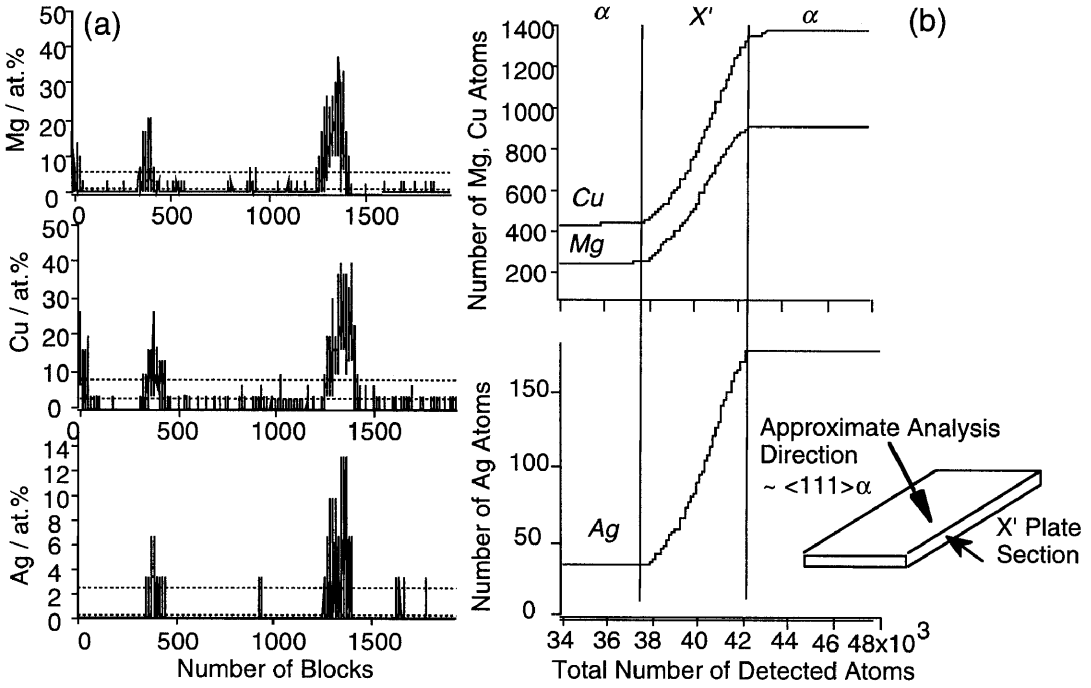

Figure 8. Atom probe analysis of Al-1.1Cu-1.7Mg-0.1Ag (at.%) alloy following ageing for 1 h. at 200 °C. (a) Concentration-depth profile and (b) Integrated concentration-depth profile showing schematic of analysis mode.

observed here seems to lie between that if the X' and the T_1 precipitate phases and it is rather similar to that of the Ω phase. Work is in progress to identify the phase, which makes an interesting addition to the microstructures featuring $\{111\}_\alpha$ precipitates through microalloying.

6. Conclusions

- The technique of APFIM is enabling an understanding of the precise atomic events associated with precipitate nucleation in aged Al alloys.
- The trace elements studied all show a preferred interaction with vacancies during or immediately after quenching from the solution treatment temperature.
- Trace amounts of Sn (Cd or In) stimulate precipitation of uniform dispersions of the phase θ' in Al-Cu alloys by providing sites, i.e. particles of Sn, Cd or In, at which heterogeneous nucleation can occur. Contrary to earlier suggestions, these elements do not segregate to the θ'/matrix interfaces during growth of this precipitate.
- Pre-precipitate atomic co-clusters of Cu and Mg are responsible for the rapid hardening reaction in Al-1.1Cu-1.7Mg (at. %) alloys aged at 150 °C.
- Cluster hardening (i.e.) hardening due to the formation of sub-nanometre atomic clusters, may represent a new hardening mechanism, applicable to (e.g.) a range of Al-Cu-Mg based alloys.
- Ag and Si modify the precipitation processes in Al-Cu-Mg alloys by modifying pre-precipitate clustering reactions during the early stages of ageing. Fine scale Mg-Ag co-clusters were detected in Al-1.1Cu-1.7Mg-0.1Ag, together with numerous Mg-rich clusters, some of which contained Cu. The addition of Si to this alloy accelerates the interaction of solute and fine scale precipitates, rich in Mg and Cu and containing traces of Ag and Si, were detected immediately following the rapid hardening reaction. Other precipitates, rich in Cu, were also observed. The formation of these various clusters and precipitates is linked to the rapid hardening reaction.
- The $\{111\}_\alpha$ X' phase was analysed by atom probe and composition in the range Cu: 0.2-0.25, Mg: 0.15-0.25 an Al:0.5-0.65 reported. Furthermore, Ag was detected in association with the precipitate. Integrated concentration-depth profiles suggest that Ag is enriched in the precipitate phase to levels as high as 5 at.%.
- An unidentified $\{111\}_\alpha$ precipitate was observed in the quinary Al-1.1Cu-1.7Mg-0.1Ag-0.3Si (at. %) alloy when aged to peak hardness at 200 °C.

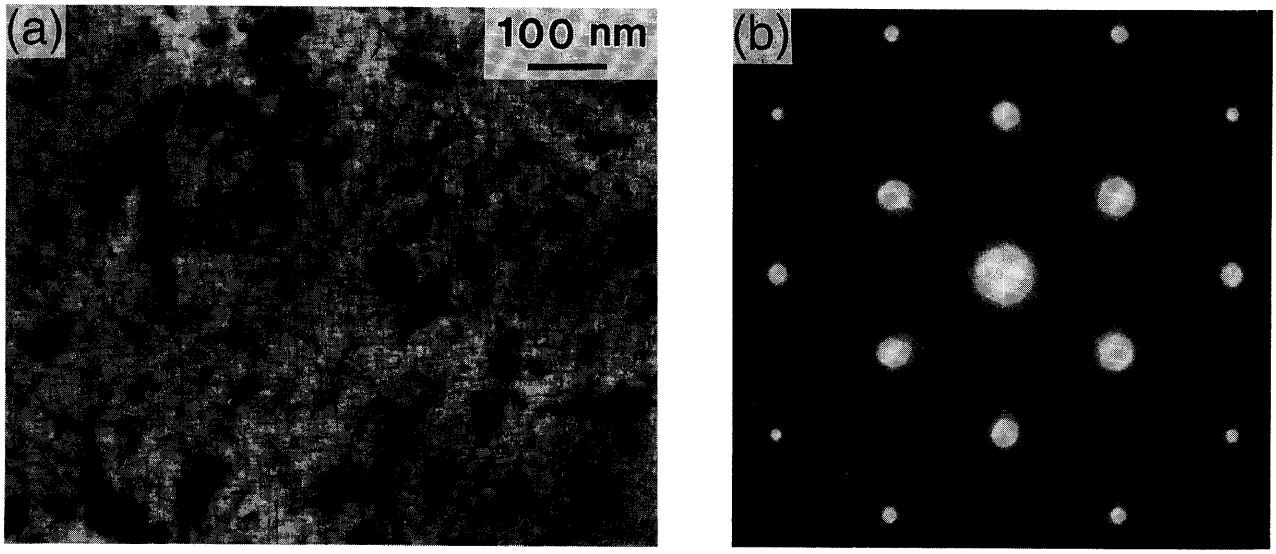

Figure 9. (a) Bright field Transmission electron micrograph and (b) $<110>_{\alpha}$ selected area electron diffraction pattern from Al-1.1Cu-1.7Mg-0.1Ag-0.3Si (at. %) alloy following ageing for 14 h. at 200 °C (peak hardness condition).

Acknowledgements

Part of this work was performed by SPR during a Japan Society for the Promotion of Science Postdoctoral Fellowship at the Institute for Materials Research (IMR), Tohoku University. Partial support from the Australian Research Council and from the Materials Engineering vacation scholarship program (CRH) is also gratefully acknowledged.

1) M.K. Miller and G.D.W. Smith, Atom Probe Microanalysis-Principles and Applications to Materials Problems (Materials Research Society, Pittsburgh, 1989).
2) J.W. Edington, Practical Electron Microscopy in Materials Science, (Van Rostrand Reinhold Co., Wokingham, **5**, 1988).
3) K. Hono, R. Okano, T. Saeda and T. Sakurai, Appl. Surf. Sci. **87/88** (1995) 453.
4) K. Hono, T. Hashizume and T. Sakurai, Surf. Sci., **266** (1992) 506.
5) H.K. Hardy, J. Inst. Metals **78** (1950-51) 169.
6) J.M. Silcock, Phil. Mag. **14** (1959) 1187.
7) H. Kimura and R. Hasiguti, Acta Metall. **9** (1961) 1076.
8) J.B.M. Nuyten, Acta Metall. **15** (1967) 1765.
9) A.Q. Khan, Trans. Japan Inst.Metals **13** (1972) 149.
10) Y. Baba, Trans. Japan Inst. Metals **10** (1969) 188.
11) J.M. Silcock, T.J. Heal and H.K. Hardy, J. Inst. Metals **84** (1955-56) 23.
12) I.J. Polmear and H.K. Hardy, J. Inst. Metals **81**, (1952-53) 427.
13) J.D. Boyd and R.B. Nicholson, Acta Metall. **19** (1971) 1101.
14) R. Sankaren and C. Laird, Mater. Sci. Eng. **14** (1974) 271.
15) M. Kanno, H. Suzuki and O. Kanoh, J. Japan Inst. Metals **44** (1980) 1139.
16) S.P. Ringer, K. Hono and T. Sakurai, Metall. Mater. Trans. **26A** (1995) 2207.
17) M. Kanno and B.L. Ou, J. Japan Inst. Light Metals **40** (1990) 672.
18) S-I Fujikawa, Proc. Conf. Sci. and Eng. of Light Metals, eds. K. Hirano et al. (Japan Inst. Light Metals, Tokyo, 1991) p.959.
19) A. Wilm, Metallurgie **8** (1911) 223.
20) H.K. Hardy, J. Inst. Metals **83** (1954-55) 17.
21) J.T. Vietz and I.J. Polmear, J. Inst. Metals **94** (1966) 410.
22) H. Lambot, Rev. Met. **47** (1950) 709.
23) Yu. A. Bagaryatsky, Doklady, Akad. Nauk SSSR **87** (1952) 559.
24) J.M. Silcock, J. Inst. Metals **89** (1960-61) 203.
25) T. Takahashi and T. Sato, J. Jap. Inst. Light Met. **35**, (1985) 41.
26) V. Radmilovic, G. Thomas, G.J. Shiflet and E.A. Starke, Scripta Metall. **23** (1989) 1141.
27) K. Hirano and K. Hono, Ann. Rev. Mater. Sci. **18** (1988) 351.
28) K. H. Westmacott, R. S. Barnes, D. Hull and R. E. Smallman, Phil. Mag. **6A** (1961) 929.
29) C. Panseri and T. Federighi, Acta Metall. **12** (1964) 272.
30) S.P. Ringer, K. Hono, I.J. Polmear and T. Sakurai, Acta Mater. **44** (1996) 1883.
31) G.A. Edwards, K. Stiller and G.L. Dunlop, Proc. 4th Int. Conf. on Aluminium Alloys - Their Physical and Mechanical Properties (ICAA4), eds. T.H. Sanders Jr. and E.A. Starke Jr. (Georgia Inst. of Tech., Atlanta, 1994).
32) I.J. Polmear, Trans A.I.M.E. **230** (1964) 1331.

33) H.D. Chopra, B.C. Muddle and I.J. Polmear, Phil. Mag. Lett. **71** (1995) 319.
34) Y. Jin, C. Li and M. Yan, J. Mats. Sci. **26** (1991) 3244.
35) J.H. Auld and J.T. Vietz, The Mech. Phase Transf. in Cryst. Solids, Inst. of Metals, London, Monograph and Report Series **33** (1969) 77.
36) R.A. Herring, F.W. Gayle and J.R. Pickens, J. Mats. Sci. **28** (1993) 69.
37) B.C. Muddle and I.J. Polmear, Acta Metall. **37** (1989) 777.
38) S.P. Ringer, K. Hono, I.J. Polmear and T. Sakuarai, Proc. Intl. Conf. on Solid-Solid Phase Transformations '94, (TMS, Warrendale, 1994) p.165.
39) J.M. Howe, Phil. Mag. Letters **70** (1994) 111.
40) Y-S Lee, S.P. Ringer , I.J. Polmear and B.C. Muddle, Proc. 4th Int. Conf. on Aluminium Alloys, eds. T.H. Sanders Jr. and E.A. Starke Jr. (Georgia Inst. of Tech., Atlanta, 1994) p. 582.
41) K. Hono, N. Sano, S.S. Babu, R. Okano and T. Sakurai, Acta Metall. Mater. **41** (1993) 829.